Spectral switches of a double slit with a movable central part in the far-field

2009 J. Opt. A: Pure Appl. Opt. 11 085410

(http://iopscience.iop.org/1464-4258/11/8/085410)

J. Opt. A: Pure Appl. Opt. **11** (2009) 085410 (6pp) doi:10.1088/1464-4258/11/8/085410

Spectral switches of a double slit with a movable central part in the far-field

Pin Han[1,3] **and Cheng-Ling Lee**[2]

[1] Institute of Precision Engineering, National Chung Hsing University, 250 Kuo Kuang Road, Taichung 402, Taiwan, Republic of China
[2] Department of Electro-Optical Engineering, National United University, Miaoli 360, Taiwan, Republic of China

E-mail: pin@dragon.nchu.edu.tw

Received 30 March 2009, accepted for publication 26 May 2009
Published 6 July 2009
Online at stacks.iop.org/JOptA/11/085410

Abstract
The far-field spectral properties for a broad-band Gaussian spectrum incident on a double slit with a movable central part are investigated. The analytic expression is first derived and some numerical examples based on it are given to illustrate the anomalous behavior of the diffracted spectrum. It is found that the important effect called spectral switches can be controlled by simply moving the central part of the double slit. This control mechanism has the merit of easier implementation than previous schemes which modulate some properties of the light source (e.g. spatial coherence or spectral bandwidth) to achieve it.

Keywords: singular optics, spectral switches, double slit with movable central part, Gaussian spectrum, Fresnel–Kirchhoff diffraction integral, red-shift, blue-shift

1. Introduction

Spectral anomalies [1–6], which are caused by the diffraction of an aperture for a polychromatic light source (or broad-band pulses), lately have gained more interest for their different applications such as lattice spectroscopy [1] or spatial-coherence spectroscopy [3]. In the past, the spectral switch phenomenon has been attributed to the singular optics effect, in which drastic spectral changes take place near some singular points with zero amplitude [5–7]. However, one of the present authors has shown that the spectral switch can exist without the phase singular points and the correct relationship between them was clarified [2]. It is found that the singularities are only the sufficient condition for the spectral switch and that the necessary condition is the oscillatory behavior of the modifier function. In this paper spectral switches with and without the singular points can both be found, and this is the first case to our knowledge. A way to utilize spectral switches for digital information and transmission in free space has been proposed [6]. Usually the 'internal mechanisms' which modulate either the spectral bandwidth or the spatial coherence of the light source are used to control the switch, but this is not an easy task [6]. In this paper, an easy scheme to control the spectral switch is suggested. We will show that it can be controlled by simply moving the central part of the aperture, which is referred to as the 'external mechanism'. Some of the predicted spectral switch effects have been verified experimentally [8–10].

[3] Author to whom any correspondence should be addressed.

2. Theory

Consider that a spatially completely coherent light, with a spectral scalar field $U'(p', \omega)$ is incident from the left upon double slit with a movable central part, as indicated in figure 1(a). This double slit has width $2a$ with a movable central obstruction (dimension a) which is centered at $(\xi, 0)$ of the incident plane, as shown in figure 1(b). Consequently, the light wave will be diffracted and arrive at the observation (or detection) plane at (x, y, z) in the far-field. The diffraction field $U(p, \omega)$ on that plane can be obtained by the Fresnel–Kirchhoff diffraction integral [11] as

$$U(p, \omega) = \frac{1}{\mathrm{j}\lambda} \int \int_{\Sigma'} U'(p', \omega) \frac{\exp(\mathrm{j}\omega r/c)}{r} \chi(\theta)\, \mathrm{d}\sigma', \quad (1)$$

where $\chi(\theta)$ is the obliquity factor, λ is the wavelength, ω is the angular frequency, c is the velocity of the light wave, and r is the distance from point $p'(x', y', 0)$ on the aperture plane

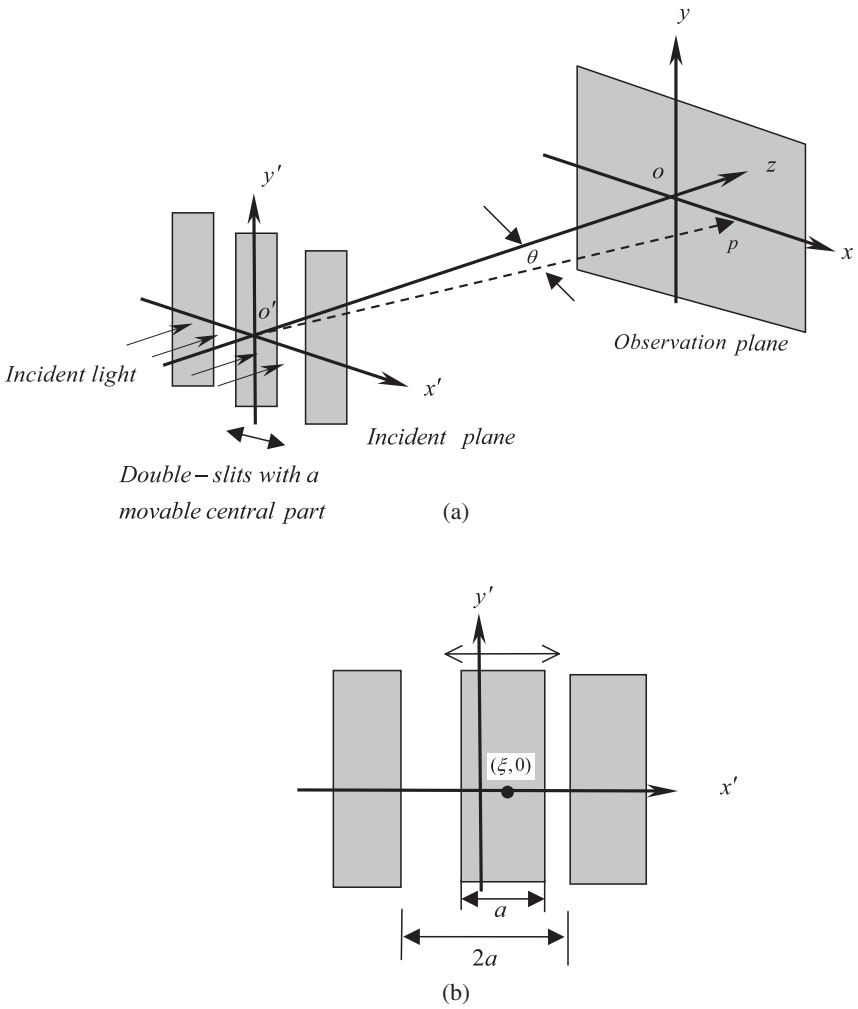

Figure 1. (a) Basic geometry. An incoming light wave from the left is incident on a double slit with a movable central part. (b) Dimensions and structures of the double slit. The movable central part is centered at $(\xi, 0)$.

to point $p(x, y, z)$ on the observation plane. As plotted in figure 1(a), the coordinate systems $x'\mathrm{o}'y'$ and $x\mathrm{o}y$ are used for the incident (aperture) plane and the observation (detection) plane, respectively. In the integral of equation (1), the notation Σ' is the aperture function and $\mathrm{d}\sigma'$ is the integration to it. Due to the symmetry property along the y' axis in our optical setup, we can limit our discussion along x', choose the observation point p along x without losing generality and designate θ as the angle between $\overline{\mathrm{o}'p}$ and optical axis $\overline{\mathrm{o}'\mathrm{o}}$ as shown in figure 1. Equation (1) is usually used for a monochromatic incident field, but it is also applicable for a broad-band pulse or polychromatic field [12], which can be superposed by a monochromatic field via the Fourier integral.

The aperture function in figure 1(b), which represents the limited area of incoming light, can be written as

$$g(x') = \Pi\left(\frac{x'}{2a}\right) - \Pi\left(\frac{x'-\xi}{a}\right), \qquad |\xi| \leqslant 0.5a \tag{2}$$

where $\Pi(x')$ is the rectangular function defined as $\Pi(x'/2a) = 1$ for $|x'| \leqslant a$ and $\Pi(x'/2a) = 0$ for $|x'| > a$; and the second term in equation (2) is the central obstruction. The Fourier transform of this aperture function $F(g(x'))$ is

$$F(g(x')) = a\{[2\mathrm{sinc}(2a\pi f_x)] - [\mathrm{sinc}(a\pi f_x)] \times \exp(-\mathrm{j}2\pi f_x\xi)\}, \tag{3}$$

where the sinc function is defined as $\mathrm{sinc}(x) = \sin(x)/x$; f_x is the spatial frequency variable. It is assumed that the incident spectral scalar field $U'(p', \omega)$ is spatially completely coherent light consisting of a single line of Gaussian profile, centered at angular frequency ω_0 with room mean square (rms) bandwidth Γ; that is,

$$U'(p', \omega) = \exp\{-[(\omega - \omega_0)]^2/2\Gamma^2\}. \tag{4}$$

Using $r \simeq [z^2 + (x - x')^2]^{1/2} \approx z + [(x^2)/2z] - (xx'/z)$ for the far-field approximation and substituting equation (4) in (1), the diffraction field $U(p, \omega)$ can be obtained as [13]

$$U(p, \omega) = \frac{1}{\mathrm{j}\lambda z}\exp\left[\mathrm{j}k\left(z + \frac{x^2}{2z}\right)\right]U'(p', \omega)F(g(x')), \tag{5}$$

where the wavenumber is written as $k = \omega/c = 2\pi/\lambda$ and the last term $F(g(x'))$ is the Fourier transform of the aperture function $g(x')$ in equation (3) with the spatial frequency $f_x =$

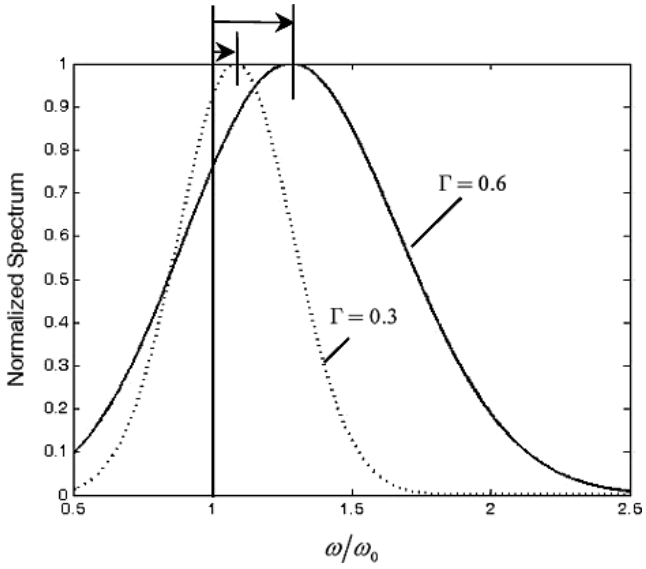

Figure 2. Spectral intensity of $I_1(0, \omega) \propto \omega^2 G(\omega)$ on axis ($\theta = 0$) for two different bandwidths $\Gamma = 0.3\omega_0$ and $0.6\omega_0$. The spectrum is always blue-shifted. As the bandwidth γ increases, the amount of the peak's shift increases. (Each curve is normalized to its maximum value.)

$x/\lambda z$. Substituting equations (3) and (4) into (5), and using the equalities $1/\lambda = \omega/2\pi c$, we have

$$U(p,\omega) = \frac{a}{\mathrm{j}z}\left(\frac{\omega}{2\pi c}\right)\exp\left[\mathrm{j}k\left(z+\frac{x^2}{2z}\right)\right] \times \exp\{-[(\omega-\omega_0)]^2/2\Gamma^2\}\cdot\{[2\mathrm{sinc}(2a\pi f_x)] - [\mathrm{sinc}(a\pi f_x)]\exp(-\mathrm{j}2\pi f_x\xi)\}. \quad (6)$$

With the relations $\sin\theta \simeq x/z$ and $f_x = \omega\cdot x/2\pi cz = \omega\sin(\theta)/2\pi c$, the spectral intensity $I(\theta,\omega)$ along the x axis with angle θ can be obtained through $I(\theta,\omega) = |U(p,\omega)|^2 = U(p,\omega)U(p,\omega)^*$ as

$$I(\theta,\omega) = A\omega^2\exp\{-[(\omega-\omega_0)]^2/\Gamma^2\} \times\{4[\mathrm{sinc}^2(a\omega\sin(\theta)/c)] + [\mathrm{sinc}^2(a\omega\sin(\theta)/2c)] - [4\mathrm{sinc}(a\omega\sin(\theta)/c)\mathrm{sinc}(a\omega\sin(\theta)/2c) \times \cos(\xi\omega\sin(\theta)/c)]\} \equiv AG(\omega)M(\theta,\omega), \quad (7)$$

where $A = a^2/(2\pi cz)^2$. $G(\omega) = \exp\{-[(\omega-\omega_0)]^2/\Gamma^2\}$ is the spectrum of the incident light source, as derived in equation (4) due to $G(\omega) = |U'(p',\omega)|^2$, and $M(\theta,\omega) = \omega^2\{4[\mathrm{sinc}^2(a\omega\sin(\theta)/c)] + [\mathrm{sinc}^2(a\omega\sin(\theta)/2c)] - [4\mathrm{sinc}(a\omega\sin(\theta)/c)\mathrm{sinc}(a\omega\sin(\theta)/2c)\cos(a\xi\cdot\sin(\theta)/c)]\}$ is called the modifier function. As indicated in equation (7), this modifier function illustrates how the spectrum of the light is modified (or modulated) as a result of diffraction at the aperture with a movable part. Equation (7) is used to give some numerical examples below, which characterize spectral anomalies (e.g. red-shift, blue-shift, spectral switches, etc) under different situations.

3. Numerical results of spectral intensity distribution

In section 3.1, we first discuss how the spectral intensity distribution changes at different observation positions along the x direction (or equivalently the angle θ). In section 3.2, the spectrum influenced by the movable central part is investigated and the scheme to perform its potential application in information encoding and transmission is introduced.

3.1. Spectral intensity distribution at different observation positions

For a double slit with the central part fixed at a position, the modifier function $M(\theta,\omega)$ depends on the observation angle θ; thus the spectral intensity distribution will change accordingly with the location. Two different cases (on axis and off axis) are discussed separately.

3.1.1. Spectral intensity distribution when $\theta = 0$ (on axis). When the observation point p is exactly at the center o of the observation plane (figure 1), the angle $\theta = 0$ is held. Therefore the equalities $\sin(\theta) = 0$ and $\mathrm{sinc}(0) = 1$, can be substituted into equation (7) to give the spectral intensity at $\theta = 0$ as

$$I(\theta = 0,\omega) = I_1(0,\omega) = A\omega^2 G(\omega). \quad (8)$$

It is found from the above equation that $G(\omega)$ now is modified by a simple function $M(\theta = 0,\omega) = \omega^2$, as shown in figure 2 for two different values of Γ. The peak of diffracted spectrum $I_1(0,\omega)$ is always blue-shifted and its amount relates to the bandwidth Γ. The amount of shift increases as the bandwidth Γ rises, as in figure 2. The maximum of the spectral intensity is at $\omega_{\max I} = 1/2[1+(1+(2\gamma)^2)^{1/2}]\omega_0$, and the amount of shift is $\Delta\omega = \omega_{\max I} - \omega_0 = 1/2[(1+(2\gamma)^2)^{1/2} - 1]\omega_0$. This behavior, in which the incident spectrum $G(\omega)$ is modified by the ω^2 term at $\theta = 0$ can also be found in other works with different aperture structures [14, 15].

3.1.2. Spectral intensity distribution when $\theta \neq 0$ (off axis). When the observation point p is not on the optical axis $z(\theta \neq 0)$, we can plot the behavior of the spectral intensity with equation (7). Since from equation (7) the resultant spectrum $I(\theta,\omega)$ is the product of the incident spectrum $G(\omega)$ and the modifier function $M(\theta,\omega)$, the behavior of $I(\theta,\omega)$ can be discussed separately according to the different properties of $M(\theta,\omega)$ as the following.

(a) *Smooth movement of the spectrum peak.* Let the detection angle start from $\sin(\theta_1) = 3.0\times10^{-4}$ for typical parameter values such as $\omega_0 = 3\times10^{15}$ rad s^{-1}, $a = 1.0$ mm, $\xi = 0.3$ mm and $\Gamma = 0.2\omega_0$; these values are used in all the following numerical examples unless specified otherwise. At this angle, as shown in figure 3(a), the modifier function is an increasing function of frequency in the neighborhood of ω_0, thus the peak of $I(\theta,\omega) \propto G(\omega)\cdot M(\theta,\omega)$ is shifted toward higher frequency; i.e., it is blue-shifted. For an larger angle at $\sin(\theta_2) = 4.4\times10^{-4}$, $M(\theta,\omega)$ is peaked at central angular frequency ω_0, as shown in figure 3(b). Since $G(\omega)$ is a symmetric function of ω and also has its maximum value at $\omega = \omega_0$, the peak of the diffracted spectrum $I(\theta,\omega)$ also occurs at this frequency. Thus the peak of the diffracted spectrum is unshifted as compared with the incident spectrum $G(\omega)$. Next, the

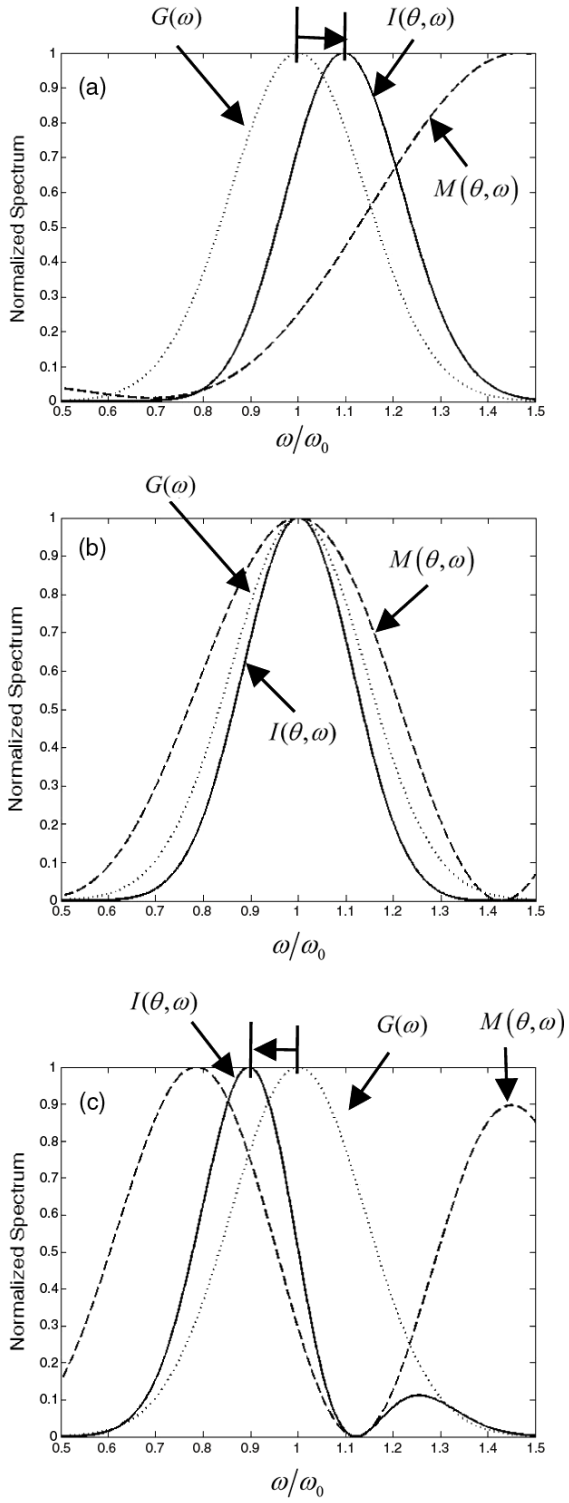

Figure 3. Normalized spectral intensity for $I(\theta, \omega)$ (solid line), $G(\omega)$ (dotted line), and $M(\theta, \omega)$ (dashed line) at different angles. (a) $\sin(\theta_1) = 3.0 \times 10^{-4}$. (b) $\sin(\theta_2) = 4.4 \times 10^{-4}$. (c) $\sin(\theta_3) = 5.6 \times 10^{-4}$. For all the following figures, the same curve styles are used consistently.

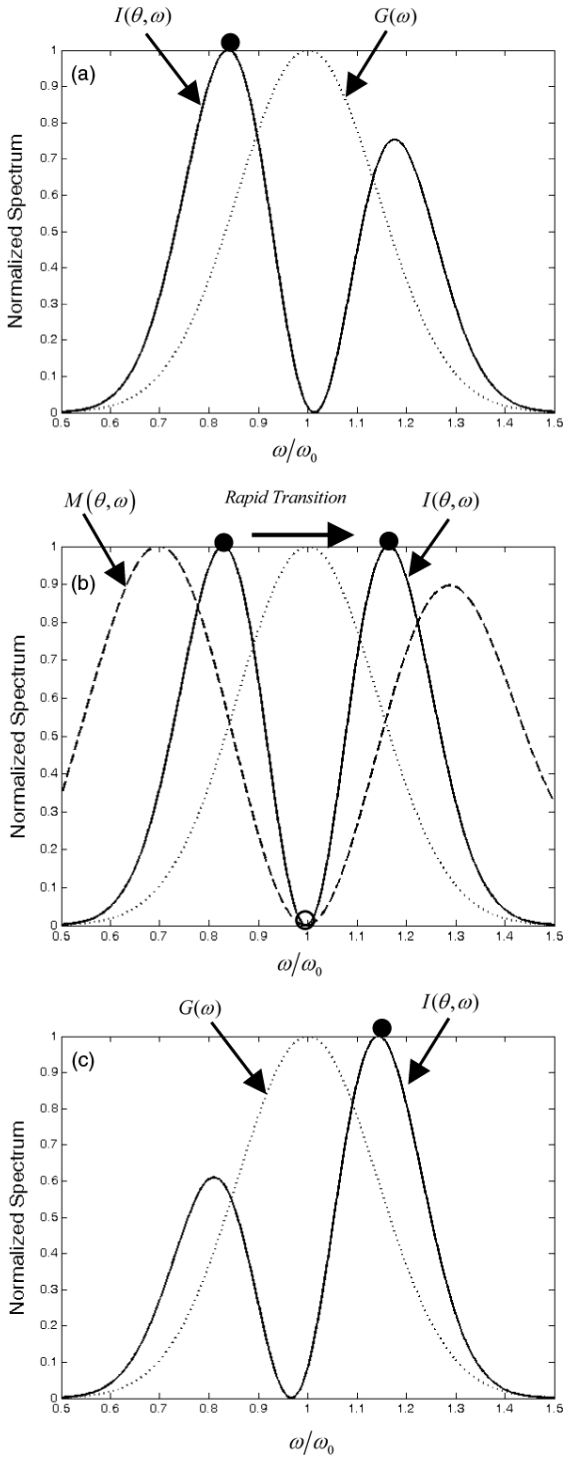

Figure 4. Normalized spectral intensity for $I(\theta, \omega)$, $G(\omega)$, and $M(\theta, \omega)$ at different angles. (a) $\sin(\theta_4) = 6.2 \times 10^{-4}$. (b) $\sin(\theta_5) = 6.305 \times 10^{-4}$. (c) $\sin(\theta) = 6.5 \times 10^{-4}$. The small solid dots in the plots indicate the positions of the maximum of the spectrum.

angle can be increased further to $\sin(\theta_3) = 5.6 \times 10^{-4}$, and as shown in figure 3(c) the modifier function at this angle is a decreasing function of frequency in the neighborhood of ω_0, thus the peak of $I(\theta, \omega)$ is shifted toward lower frequency; i.e., it is red-shifted.

(b) *Sudden change of the spectrum peak (spectral switch).* If the angle keeps increasing to $\sin(\theta_4) = 6.2 \times 10^{-4}$, as shown in figure 4(a), the main (left) peak of $I(\theta, \omega)$

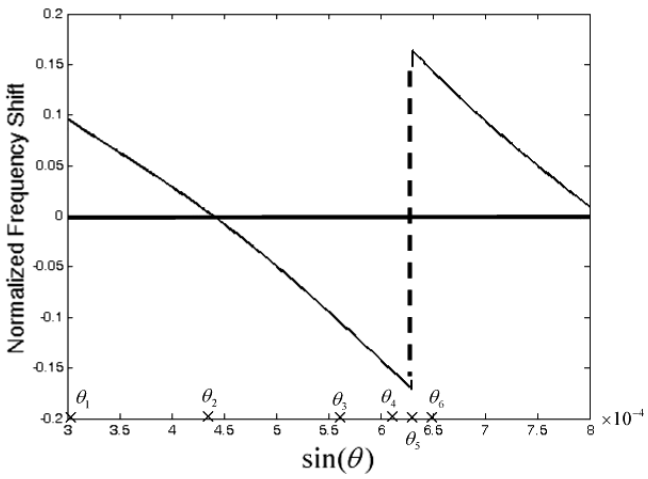

Figure 5. Plot of the normalized frequency shift Ω as a function of $\sin(\theta)$ for the parameter values $\omega_0 = 3 \times 10^{15}$ rad s^{-1}, $a = 1$ mm, $\xi = 0.3$ mm and $\gamma = 0.2$. The six angles indicated on the x axis from θ_1 to θ_6 marked with '$\times$' correspond to the picked angles for figures 3(a)–(c) and figures 4(a)–(c) respectively. It is found that at θ_2 there is no shift for the spectrum's peak ($\Omega = 0$ as in figure 3(b)) and at θ_5 there is a discontinuous jump (spectral switch) as in figure 4(b).

is still red-shifted, but the height of the right peak also increases, as compared with figure 3(c). The small solid dots in the plots indicate the position of the maximum of the spectrum. Next, for a little bigger value of $\sin(\theta_5) = 6.305 \times 10^{-4}$, figure 4(b) shows that the two peaks reach the same height. This critical angle is called θ_s and the subscript means the spectral switch. As illustrated on the figure, the two peaks are divided by a phase singular point (marked with a small circle on the horizontal axis near $\omega = \omega_0$), and at this frequency the amplitude of the spectrum is zero, which makes the phase there singular. However, it will be shown in section 3.2 that the equal heights for the two peaks can appear without resorting to the singular point. When the value of θ increases a little to $\sin(\theta_6) = 6.5 \times 10^{-4}$, figure 4(c) shows that the right peak now is the main peak and the blue-shift occurs. This demonstrates the existence of the spectral switch at θ_s and the spectral shift has a sudden change (in (c)) from red-shift (in (a), $\theta < \theta_s$) to blue-shift (in (c), $\theta > \theta_s$) in the vicinity of θ_s. For better explaining the behavior of spectral behavior from above discussion, the normalized frequency shift concept is used and defined as

$$\Omega = (\omega_p - \omega_0)/\omega_0, \tag{9}$$

where ω_p is the frequency at which the diffracted spectrum peaks. This quantity is plotted as a function of $\sin(\theta)$ in figure 5 and the angles indicated on the x axis from θ_1 to θ_6 marked with '$\times$' correspond to those angles for figures 3 and 4. It is obvious from this plot that at θ_2 (see figure 3(b)) there is no shift for the spectrum's peak ($\Omega = 0$), and near θ_5 (or θ_s) (see figure 4(b)) there is a discontinuous jump for Ω (spectral switch) from red-shift (figure 4(a)) to blue-shift (figure 4(c)).

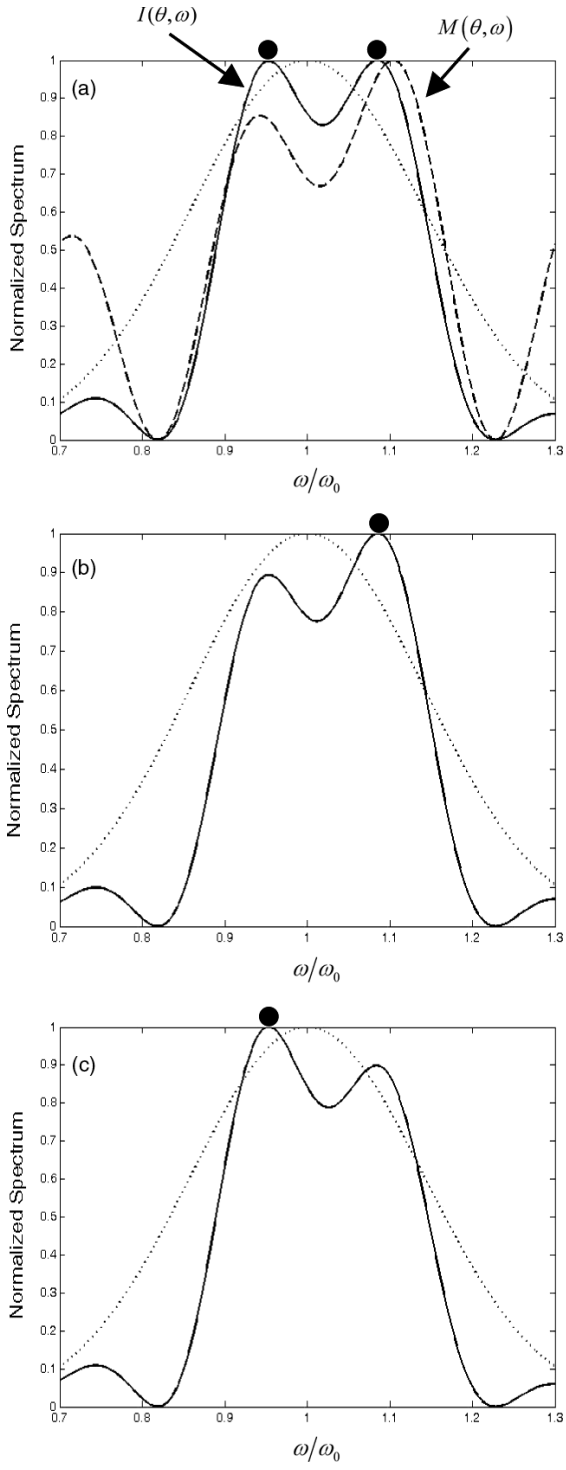

Figure 6. Normalized spectra for $G(\omega)$ and $I(\theta, \omega)$ for different movement amounts of the central part. (a) $\xi = 0.3$ mm. (b) $\xi = 0.29$ mm. (c) $\xi = 0.31$ mm. It is found that in (a), $I(\theta, \omega)$ splits into two peaks with equal heights and the peak is blue-shifted (b) or red-shifted (c) by slight movement of the central part to the left or right respectively.

3.2. Spectral switch control by the movement of the central part

Now we can consider how the diffracted spectrum is affected by the movement of the central part of the double slit with

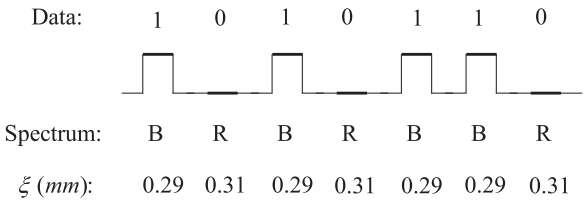

Figure 7. Illustration for the data encoding and information transmission by controlling the movement of the central part. The blue-shift (B, for short) is associated with a bit of information such as '1' and the red-shift (R, for short) is associated with a bit of '0'.

equation (7). Due to the complicated form and behavior of the modifier function $M(\theta, \omega)$ in equation (7), it is found that at some particular angle (e.g. $\sin(\theta) = 1.535 \times 10^{-3}$ in figure 6(a)) $M(\theta, \omega)$ can again redistribute $I(\theta, \omega)$ into two peaks with equal heights, but without the singular point between them. Comparing figure 6(a) with 4(b), it is found that the singular point is not always needed for the spectral switch. However, the oscillatory behavior of $M(\theta, \omega)$ shows up in both cases, and this is why the authors claim that the oscillating property of the modifier function is the real cause and the necessary condition for the spectral switch [2]. Under this situation, the central part is moved slightly from its original position ($\xi = 0.3$ mm) to the left ($\xi = 0.29$ mm) or to the right ($\xi = 0.31$ mm) and the spectral intensity is plotted in figures 6(b) and (c) respectively. The sudden changes from blue-shift to red-shift of the spectrum maximum are obvious in these two figures; thus the central part movement can control the spectral switch.

The spectral switches and diffracted spectrum peak shift have been utilized in information encoding and transmission in free space, and in that work the rms bandwidth or spatial coherence of the incident field is used to modulate the incident light (this can be called the internal mechanism), which is not an easy task to perform [6]. In this paper, we propose another scheme to achieve the spectral switch by simply moving the central part of a double slit slightly while the properties of the incident light source do not need any changes, which is referred to as the external mechanism. Referring to figure 7, it is assumed that there is a set of data as shown in the first row of figure 7 needed to be transmitted to a position p which makes an angle θ from the optical axis $\overline{o'o}$. It is noted that any specific transmitting angle at which the spectral switch can occur always can be found through the suitable selection of the parameters ω_0, Γ, a, and ξ. We designate blue-shift and red-shift as a bit of '1' or '0' respectively (the notations B and R are used to indicate the blue-shift and red-shift in the row under the data plot). Thus by properly adjusting the translation of the central part, the blue-shift or red-shift of the spectrum's peak can be controlled accordingly. For the calculation example in figure 6, it is found that, when $\xi = 0.29$ mm $\xi = 0.31$ mm, the blue-shift ($\omega_p = 1.08\omega_0$) and red-shift ($\omega_p = 0.95\omega_0$) can be produced respectively, where ω_p is the frequency at which the spectrum of the diffracted spectrum peaks. Under this situation, the data can be encoded and transmitted through the movement of the central part, as shown in the bottom row in figure 7. Thus this method is direct and easier to implement, and no incident light field properties need to be modulated to control the spectral switches.

4. Conclusion

In this paper the far-field spectral anomalies of a light source with Gaussian spectrum incident on a double slit with a movable central part are studied. The analytical expression for spectral intensity distribution is obtained and some numerical examples based on it indicate the spectral switches and the spectrum peak's blue-or red-shift behavior. The figures also illustrate how the observation position and movement of the central part of the double slit affect the diffracted spectrum. It is noted that the spectral switches can exist without the singular points and the necessary condition is the oscillatory behavior of the modifier function. Consequently, we offer another scheme which can control the spectral switches by adjusting the movement of the central part and show how it can be applied to information encoding and transmission in free space. This scheme has the benefit of easy implementation without changing the properties of the light source.

Acknowledgments

This study was supported by the National Chung Hsing University, Taiwan, ROC. The authors would also like to thank their colleagues for thoughtful comments and useful suggestions. This work was also supported by the NSC of ROC under contract no NSC 97-2622-E-005-004-CC3.

References

[1] Han P 2009 *Opt. Lett.* **34** 1303
[2] Han P 2009 *J. Opt. A: Pure Appl. Opt.* **11** 015708
[3] Wolf E and James D F V 1996 *Rep. Prog. Phys.* **59** 771–818
[4] Gbur G, Visser T D and Wolf E 2002 *Phys. Rev. Lett.* **88** 013901
[5] Foley J and Wolf E 2002 *J. Opt. Soc. Am.* A **19** 2510–6
[6] Pu J, Cai C and Nemoto S 2004 *Opt. Express* **12** 5131–9
[7] Soskin M S and Vasnetsov M V 2001 Singular optics *Progress in Optics* vol 42, ed E Wolf (Amsterdam: Elsevier) p 219
[8] Qu B, Pu J and Chen Z 2007 *Opt. Laser Technol.* **39** 1226–30
[9] Kandpal H C 2001 *J. Opt. A: Pure Appl. Opt.* **3** 296–9
[10] Popescu G and Dogariu A 2002 *Phys. Rev. Lett.* **88** 183902
[11] Hecht E 2002 *Optics* 4th edn (New York: Addison-Wesley) p 511
[12] Goodman J W 1996 *Introduction to Fourier Optics* 2nd edn (New York: McGraw-Hill) p 53
[13] Iizuka K 2002 *Elements of Photonics* (New York: Wiley) p 11
[14] Han P 2008 *J. Opt. A: Pure Appl. Opt.* **10** 035003
[15] Han P 2009 *J. Opt. Soc. Am.* A **26** 473–9